PARTICLE SIZE DISTRIBUTION OF AGGLOMERATED CRYSTAL PRODUCT FROM A CONTINUOUS CRYSTALLIZER

Jiří HOSTOMSKÝ

Institute of Inorganic Chemistry,
Czechoslovak Academy of Sciences, 160 00 Prague 6

Received April 11th, 1986

Relationships have been derived for the particle size distribution in a continuous crystallizer operating in a steady-state regime, where agglomeration of the primarily generated crystalline particles takes place. The derivation was made for a constant kinetic coefficient of agglomeration (independent of the particle size) and for a negligible particle growth rate. The relationships are used to interpret the particle size distribution of calcium carbonate precipitated from 0·2 mol . . dm^{-3} solutions of calcium chloride and sodium carbonate in a laboratory continuous crystallizer. Anomalous shapes of the size distributions of small particles frequently observed in continuous crystallizers are discussed in terms of the agglomeration phenomenon.

Microscopic observations of products from both continuous and batch crystallizers have indicated that crystal agglomeration significantly affects the granulometric composition of the product. In agglomeration separate, previously formed crystalline particles combine and, consequently, the formal particle growth rate, expressed for example as the rate of change of the mean particle size, is substantially higher than the growth rate of the crystal surface area (normal to the surface) given by the transfer of the solute from solution to the solid phase. Agglomeration significantly affects the particle size distribution of the crystal product and the separation of the product from the mother liquor. At high levels of supersaturation, crystal agglomeration occurs very frequently, not only in precipitation of sparingly soluble substances[1-3], but also with readily soluble substances such as potassium chloride[4] and potassium aluminium sulphate[5-7].

It is more convenient to study agglomeration in the steady-state flow system than in the batch arrangement, where the solution supersaturation, the rates of the various partial processes and the crystal size distribution all vary with time. There are a large number of papers dealing with the theoretical solution of the variation in the particle size distribution with time for agglomeration in the batch arrangement[8-12]. In contrast, no theoretical relationships are available in the literature for particle agglomeration in the steady-state flow system. In the present paper, we shall derive a simple variant of the relationships for a continuous crystallizer and compare the derived equations with experimental results obtained for precipitation of calcium

carbonate. We shall also show that agglomeration may provide the basis for interpreting the frequently observed marked positive deviations from expected values for the distribution of small particles in continuous crystallizers.

THEORETICAL

Suppose that particles of a constant initial volume v_0 are generated continuously in a well-stirred continuous crystallizer operating in a steady-state regime and that these particles combine with one another and/or with previously formed particle agglomerates. Let agglomeration be the only process responsible for changes in the particle size distribution, *i.e.* we shall neglect agglomerate breakage and particle growth due to mass transfer from solution to the solid phase. The described model system may be exemplified by precipitation crystallization in a continuous crystallizer where close to the inlet of the concentrated solution there is a small zone with a high level of supersaturation in which nucleation occurs and the nuclei born grow very rapidly up to the volume v_0, thus relieving almost completely the state of supersaturation. The particles of volume v_0 then enter the bulk of the well-stirred crystallizer, where they solely agglomerate.

We shall characterize the rate of agglomeration by the agglomeration coefficient, k_a, defined in terms of the distribution function of particle volumes, $f(v)$, as follows. Let $f(v)\,\mathrm{d}v$ be the number of particles of volume v to $(v + \mathrm{d}v)$ *per* unit volume of suspension; then $k_a f(u) f(v)\,\mathrm{d}u\,\mathrm{d}v$ is the number of agglomeration collisions between particles of volume u to $(u + \mathrm{d}u)$ and those of volume v to $(v + \mathrm{d}v)$ *per* unit time and unit volume of suspension. In the derivation below, we assume for simplicity that the agglomeration coefficient k_a is constant, independent of the particle volume (see also Results and Discussion).

The steady-state population balance for particles of volume v is

$$\tfrac{1}{2}k_a \int_{v_0}^{v-v_0} f(u) f(v-u)\mathrm{d}u - k_a \int_{v_0}^{\infty} f(u) f(v)\mathrm{d}u - f(v)/\bar{t} + \dot{N}\delta(v - v_0) = 0, \qquad (1)$$

where $\dot{N}$ is the rate of generation of particles of volume v_0 *per* unit volume of suspension, $\bar{t}$ is the mean retention time of suspension in the crystallizer, and $\delta(v - v_0)$ is the Dirac impulse function. The first and second terms in Eq. (*1*) describe, respectively, the increase and decrease in the number of particles of volume v due to agglomeration, the third term represents the decrease in the number of particles as the suspension comes off the crystallizer, and the last term gives the contribution from particle nucleation, which is nonzero only for $v = v_0$. Equation (*1*) represents the deterministic description of the agglomeration process in the continuous crystallizer. Thus, assuming a large number of particles in the system, we neglect the stochastic

character of the agglomeration collisions and of the outflow of the particles from the crystallizer[13].

Integrating the second term in Eq. (1), we obtain

$$k_a \int_{v_0}^{\infty} f(u) f(v)\, du = k_a f(v) \int_{v_0}^{\infty} f(u)\, du = k_a f(v)\, M_0\,, \tag{2}$$

where M_0 is the zeroth moment of the distribution $f(v)$, *i.e.* the total number of particles in unit volume of suspension. The particle number M_0 is obtained from a balance equation for the total number of particles in unit volume of suspension in the crystallizer,

$$-\tfrac{1}{2} k_a M_0^2 - M_0/\bar{t} + \dot{N} = 0\,, \tag{3}$$

where the expression $\frac{1}{2} k_a M_0^2$ represents the number of binary agglomeration collisions *per* unit volume and unit time (one particle is lost in each collision). This equation is also obtained by integration of Eq. (1) within the limits v_0 and ∞. Equation (3) is useful in that it permits the total number of particles in unit volume of suspension to be calculated from the kinetic parameters k_a and $\dot{N}$, and the retention time $\bar{t}$ (without the knowledge of the distribution $f(v)$):

$$M_0 = [(2k_a \dot{N} \bar{t}^2 + 1)^{1/2} - 1]/k_a \bar{t}\,. \tag{4}$$

The total number of particles, M_0, can be compared with the total number of particles which would be present in unit volume of suspension if no agglomeration occurred, *i.e.* $\dot{N}\bar{t}$ (a unit volume of suspension stays in the crystallizer for an average time $\bar{t}$ in which $\dot{N}\bar{t}$ particles of volume v_0 are generated; see also Eq. (3) for $k_a = 0$). The ratio of the numbers of particles in unit volume of suspension with and without agglomeration is

$$M_0/\dot{N}\bar{t} = [(2a + 1)^{1/2} - 1]/a\,, \tag{5}$$

where

$$a = k_a \dot{N} \bar{t}^2\,. \tag{6}$$

The reciprocal of this ratio is the average number of particles that comprise an agglomerate.

The integral equation (1) can be solved by taking the Laplace transformation

$$\tfrac{1}{2} k_a F^2 - k_a M_0 F + \dot{N} \exp(-v_0 p) - F/\bar{t} = 0\,, \tag{7}$$

where F is the Laplace transform of distribution $f(v)$:

$$F = \int_0^\infty f(v) \exp(-pv)\, dv \tag{8}$$

(the $f(v)$ distribution is equal to zero in the interval $(0, v_0)$). Rearrangement of Eq. (7) gives

$$F = \frac{(1 + 2a)^{1/2}}{k_a \bar{i}} \left\{1 - \left[1 - \frac{a}{a + 1/2} \exp(-v_0 p)\right]^{1/2}\right\}. \tag{9}$$

After replacing the expression under the radical in Eq. (9) by a Taylor's series, we take the inverse transformation

$$f(v) = \frac{1 \,.\, 3 \,.\, 5 \,.\, \ldots \,.\, (2i - 3)}{2^i i!} \frac{(1 + 2a)^{1/2}}{k_a \bar{i}} \left(\frac{a}{a + 1/2}\right)^i \delta(v - iv_0), \tag{10}$$

where $i = 1, 2, 3 \ldots$ (for $v \neq iv_0$, we have $f(v) = 0$). The factorial expression in Eq. (10) may be approximated by

$$\frac{1 \,.\, 3 \,.\, 5 \,.\, \ldots \,.\, (2i - 3)}{2^i i!} \approx \frac{1}{2} \pi^{-1/2} i^{-3/2}. \tag{11}$$

This approximation has been derived on the basis of Stirling's formula and holds with sufficient accuracy for $i \geqq 10$ (the error of the approximation is 3·8% for $i = 10$, 1·3% for $i = 30$, and 0·63% for $i = 60$). So far we have considered agglomeration of elementary particles of volume v_0 or of size corresponding to a multiple of v_0, and the distribution $f(v)$ is therefore defined by Eq. (10) only at discrete points $v = iv_0$ (where the Dirac functions are nonzero). If the particle volume v is greater than about $10v_0$, the distribution can be considered as a continuous function of v:

$$f(v) = \left[\frac{(1 + 2a)\, v_0}{4\pi}\right]^{1/2} \frac{[a/(a + 1/2)]^{v/v_0}}{k_a \bar{i} v^{3/2}}. \tag{12}$$

Equation (12) is obtained by inserting Eq. (11) into (10), integrating between the limits $(i - 0{\cdot}5)\, v_0$ and $(i + 0{\cdot}5)\, v_0$, and dividing by v_0, *i.e.* by the width of the integration interval. From Eq. (12) it follows that the dimensionless distribution $f(v)/f(v_0)$ depends only on the volume ratio v/v_0 and the dimensionless parameter $a = k_a \bar{N} \bar{i}^2$:

$$f(v)/f(v_0) = [a/(a + 1/2)]^{v/v_0} (v/v_0)^{-3/2}. \tag{13}$$

We shall now turn our attention from the particle volume distribution $f(v)$ to the more frequently used particle size distribution, $n(L)$. The symbol $n(L)\, dL$ will denote

the number of particles in unit volume of suspension which have a characteristic linear dimension L to $(L + \mathrm{d}L)$. Since

$$f(v)\,\mathrm{d}v = n(L)\,\mathrm{d}L, \tag{14}$$

Eq. (*12*) can be transformed to

$$n(L) = \frac{3}{2}\left[\frac{(1 + 2a)}{\pi}\right]^{1/2} \frac{[a/(a + 1/2)]^{L^3/L_0^3}}{k_a \bar{t}} \frac{L_0^{3/2}}{L^{5/2}}, \tag{15}$$

where L_0 is the characteristic dimension corresponding to the elementary volume v_0. The slope of the semilogarithmic ln $n(L)$ *versus* L plot is

$$d[\ln n(L)]/\mathrm{d}L = -5/2L + (3L^2/L_0^3) \ln [a/(a + 1/2)]\,. \tag{16}$$

Equation (*16*) indicates that the semilogarithmic plot of the distribution $n(L)$ is a steeply falling curve for small particles. As L rises, the absolute value of the slope gradually decreases until an inflexion point with the coordinate

$$L_{\text{inflex}} = L_0\{(12/5) \ln [(a + 1/2)/a]\}^{-1/3} \tag{17}$$

is reached, whereupon the curve resumes its decline with increasing absolute value of slope. The slope in the inflexion point is $-5{\cdot}02L^{-1} \ln [(a + 1/2)/a]^{1/3}$. For high values of parameter a (for example, for the typical values $k_a = 10^{-7}$ cm^3/s, $\dot{N} = 10^4$ cm^{-3} s^{-1}, and $\bar{t} = 1\,000$ s, Eq. (*6*) gives $a = 1\,000$), the inflexion point may not be found experimentally because it lies within the range of very small (unmeasurable) values of the $n(L)$ distribution.

The logarithmic ln $n(L)$ *versus* ln L plot is initially (for small L) a straight line of slope $\mathrm{d}\ln n(L)/\mathrm{d}\ln L$ close to $-2{\cdot}5$, because the second term on the right-hand side of Eq. (*16*) multiplied by L is insignificant at low values of L (see Fig. 1). The slope of $-2{\cdot}5$ of the logarithmic plot, *i.e.* a $-2{\cdot}5$-power law for $n(L)$ as a function of L, was predicted by Friedlander[14] on the basis of dimensional analysis for the limiting case – in the nomenclature used in this paper – of an infinite retention time of a suspension in a crystallizer, *i.e.* for $a \to \infty$.

EXPERIMENTAL

Particle size distributions were measured for calcium carbonate precipitated at 25°C from 0·2 mol . . dm^{-3} solutions of calcium chloride and sodium carbonate. Under the given conditions, the major product is the metastable modification vaterite[15]. Filtered solutions of $CaCl_2$ and Na_2CO_3 were drawn with a metering pump from stock bottles through capillaries into a continuous crystallizer consisting of a thermostatted glass vessel of 160 cm^3 capacity with an outlet tube

located 1 cm below the surface of the suspension and another outlet tube at the bottom of the vessel. The suspension was stirred with a standard impeller with six inclined blades, using a stirrer speed of 500 or 260 rpm. When a minimum of ten times the mean retention time of the suspension in the vessel had elapsed, samples of the suspension were withdrawn, through both the outlets, for granulometric analysis. No difference was found between the distributions of the two samples. In order to prevent any additional agglomeration, the suspension sample (a maximum of 1 cm^3) was placed in a cell with 500 cm^3 of a solution saturated with calcium carbonate and containing the same amount of NaCl as the entering sample. The filtrate of the mother liquor from the preceding experiments was used for this purpose. The particle size distribution was measured by a Fritsch Analysette 20 Photosedimentometer (F.R.G.), which determines the decrease in the optical density of the initially homogeneous suspension settling down in the cell. The result of the measurement is the cumulative particle area distribution as a function of the particle size L (Stokes' diameter). If $S(L)$ is the percentage of crystals in suspension which are smaller than L, then $L^{-2}[\mathrm{d}S(L)/\mathrm{d}L]$ represents a quantity proportional to the particle number distribution $n(L)$. The mass balance for the crystallization (assuming spherical particles and 100% yield of $CaCO_3$) gives

$$n(L) = 6M_{CaCO_3}(c/2 - c_{eq})\,[\mathrm{d}S(L)/\mathrm{d}L] \Big/ \left[\pi L^2 \varrho_c \int_0^{100} L\,\mathrm{d}S(L)\right], \qquad (18)$$

where c is the molar volumetric concentration of the equimolar solutions of $CaCl_2$ and Na_2CO_3 c_{eq} is the solubility of $CaCO_3$, M_{CaCO_3} is the molar mass, and ϱ_c is the specific mass of the particles. The derivatives $\mathrm{d}S(L)/\mathrm{d}L$ as functions of the particle size L were obtained by successive polynomial regression of sections of the $S(L)$ versus L curve.

RESULTS AND DISCUSSION

Microscopic observation of products from calcium carbonate precipitation under the conditions specified in Table I revealed that most of the solid phase was made up of fairly compact crystal agglomerates. A semilogarithmic plot of the particle size distribution, $\log n(L)$, *versus* the characteristic dimension L generally exhibits the shape shown in Fig. 2, which differs from the linear $\log n(L)$ *versus* L plot for the ideal continuous crystallizer with a constant particle growth rate (without agglomeration)[16]. In contrast, the $\log n(L)$ *versus* $\log L$ plot is a straight line for small particles (Fig. 3), with a slope close to $-2{\cdot}5$ (Table I). The length of the linear portion of the $\log n(L)$ *versus* $\log L$ curve increases with decreasing mean retention time of the suspension in crystallizer, *i.e.* with increasing supersaturation of the solution in the crystallizer (experiments 1 to 3 in Table I).

An attempt was made to evaluate the particle growth rate, $\dot{L}$, by the conventional method[16] from slopes of $\log n(L)$ *versus* L plots in the region of larger particles for which the dependence is at least approximately linear (Fig. 2). So obtained growth rates were compared with values of the quantity $L_{50}/2{\cdot}674\bar{t}$, where the dimension L_{50} is one for which the cumulative surface area of particles with dimensions $L \leqq L_{50}$ equals one half of the total particle surface area. Thus, the L_{50} dimension can be read from the plot of $S(L)$ *versus* L obtained by photosedimentation measurement.

The numerical coefficient 2·674 is given by the equation[16]

$$S(L_{50}) = 100[1 + L_{50}/\dot{L}\bar{t} + \tfrac{1}{2}(L_{50}/\dot{L}\bar{t})^2] \exp(-L_{50}/\dot{L}\bar{t}) = 50\,, \qquad (19)$$

whose solution is

$$L_{50}/\dot{L}\bar{t} = 2{\cdot}674\,. \qquad (20)$$

TABLE I

Experimental conditions and evaluated particle size distributions

Experiment	$\bar{t}$ min	Stirrer speed min^{-1}	L_{max}[a] μm	s[b]	$\dot{L}$ μm/min	$L_{50}/2{\cdot}674\bar{t}$ μm/min
1	6	500	20	−3·3	0·96	0·30
2	18	500	11	−2·5	0·71	0·39
3	36	500	8	−2·1	0·51	0·23
4	6	260	17	−2·4	0·77	0·47

[a] The upper bound on the linearity of the log $n(L)$ *versus* log L plot; [b] the slope of the linear portion of the log $n(L)$ *versus* log L plot.

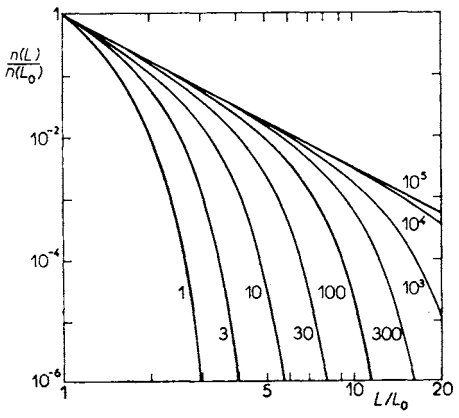

FIG. 1

Logarithmic plot of the particle size distribution according to Eq. (*15*). The figure on each curve indicates the value of the parameter $a = k_g\dot{N}\bar{t}$

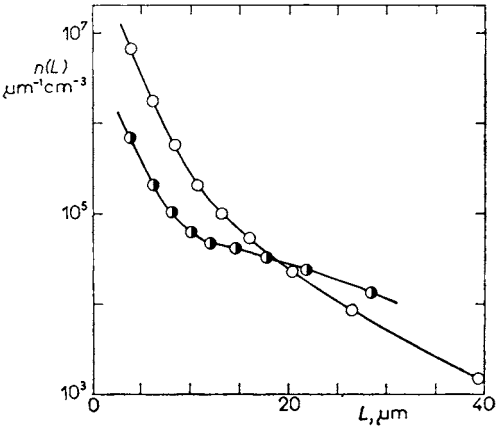

FIG. 2

Semilogarithmic plot of the particle size distribution for $CaCO_3$. ○ experiment 1; ◑ experiment 2

In Table I one sees that the growth rates determined by the two approaches differ. This is expected because in determining L_{50} an important role is played by small particles, whose contribution to the total surface area is substantially greater than would correspond to a linear extrapolation (in the plot of log $n(L)$ *versus* L) from the region of large particles.

The particle size distribution of the product was also plotted in the z–L coordinate system, where z is related to $M(L)$, the mass percent of particles larger than L, by the equation[16]

$$M(L) = 100(1 + z + z^2/2 + z^3/6) \exp(-z) . \qquad (21)$$

For the ideal continuous crystallizer, the plot is a straight line of slope $1/\dot{L}\tilde{\imath}$ passing through the origin. As seen in Fig. 4, experimental distributions plotted in this coordinate system lie on curves with positive intercepts on the $M(L)$ axis, as in papers of Nývlt and coworkers[5,7], who studied agglomeration of $KAl(SO_4)_2.12\,H_2O$ during precipitation and cooling crystallization in a continuous crystallizer.

The experimentally obtained slopes of the linear portions of the log $n(L)$ *versus* log L plots, which are close to $-2{\cdot}5$, correspond – according to the theoretical part of this paper – to agglomeration growth of particles in a continuous crystallizer at a constant agglomeration coefficient (independent of the size of agglomerating particles) and high values of the dimensionless parameter a (see Fig. 1). For experiment 1, the agglomeration coefficient determined on the basis of Eq. (*15*) from experimental distribution $n(L)$ is $k_a = 9{\cdot}4 \,.\, 10^{-10}$ cm^3/s. When determining k_a for

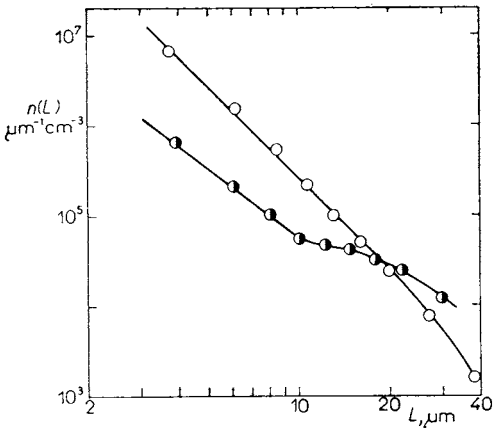

FIG. 3

Logarithmic plot of the particle size distribution for $CaCO_3$. ○ experiment 1; ◐ experiment 2

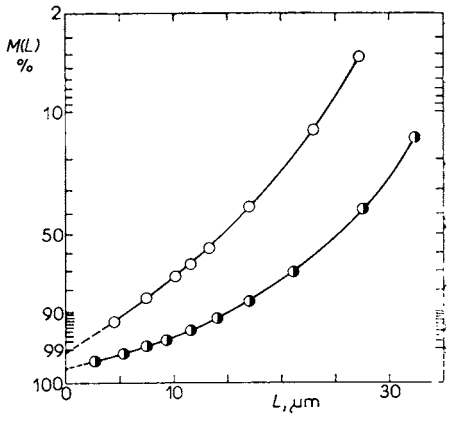

FIG. 4

Cumulative particle mass distribution for $CaCO_3$. ◑ experiment 3; ○ experiment 4

a given distribution $n(L)$, we need not know the initial size of agglomerating particles, L_0, provided that $a \gg 1$. If, for example, distribution values n_1 and n_2 for particle sizes L_1 and L_2 are known, the agglomeration coefficient k_a is equal, according to Eq. (*15*), to

$$k_a = \tfrac{3}{2}[\pi(-\ln q)]^{-1/2}\, q/(n_1 \bar{i} L_1)\,, \tag{22}$$

where

$$q = [(n_2/n_1)\,(L_2/L_1)^{5/2}]^{L_1^3/(L_2^3 - L_1^3)}\,. \tag{23}$$

Thus, L_0 does not appear in Eqs (*22*) and (*23*). Its knowledge is, however, necessary for determining the quantities a, M_0, and $\dot{N}$. Nakai and Nakamaru[17] estimated the size of $CaCO_3$ particles formed immediately on combining 0·058 to 0·25 mol . . dm^{-3} equimolar solutions of Na_2CO_3 and $CaCl_2$ to be 0·22 to 0·3 μm. Microscopic observations in their work indicated that the size of the smallest $CaCO_3$ particles was less than 1 μm. With $L_0 = 0{\cdot}3$ μm and $k_a = 9{\cdot}4 \,.\, 10^{-10}$ cm^3/s for experiment 1, Eq. (*15*) yields the dimensionless parameter $a = 1{\cdot}14 \,.\, 10^5$, and Eq. (*4*) gives the total number of particles in unit volume of suspension as $M_0 = 1{\cdot}41 \,.\, 10^9$ cm^{-3} and the growth rate of primary particles as $\dot{N} = 9{\cdot}4 \,.\, 10^8$ $cm^{-3}\, s^{-1}$.

According to the present model of agglomeration in a continuous crystallizer (constant primary particle size; agglomeration coefficient independent of particle size; and zero growth of particles), the absolute value of the slope of the log $n(L)$ *versus* log L plot should be greater than, or equal to, 2·5. In experiments 3 and 4 (Table I), however, the absolute values of the slope are somewhat lower than 2·5. This may be explained in that in a real system there is still some growth of particles as a result of mass transfer from solution to the solid phase. Should the particle size distribution in a continuous crystallizer be determined only by particle growth at a constant rate $\dot{L}$, it would be given by[16]

$$n(L) = n_0 \exp(-L/\dot{L}\bar{i})\,, \tag{24}$$

and the slope dlog $n(L)$/dlog L would be equal to $-L/\dot{L}\bar{i}$: thus, for $L = 0$, it would be zero, for $L = \dot{L}\bar{i}$ (numerical mean particle size), -1, decreasing further linearly with increasing L. For the general case where nucleation, growth and agglomeration of particles occur simultaneously, the particle size distribution is obtained by numerical solution of population balance (*1*) extended to include the growth term $\mathrm{d}[\dot{v}f(v)]/\mathrm{d}v$, where $\dot{v}$ is the rate of change of the particle volume as a result of growth. The experimental slopes of the linear plots of log $n(L)$ *versus* log L also indicate that the assumption of constant agglomeration coefficient k_a (independent of particle size) provides a better agreement between theoretical and experimental values of the slope than does the assumption of size-dependent agglomeration coefficient. For example, the relation derived by Saffman and Turner[18] for the collision coefficient

of spherical particles of diameters L_1 and L_2 under the conditions of isotropic turbulence,

$$k_a = \text{constant}\,(L_1 + L_2)^3\,, \tag{25}$$

would lead, as can be shown by the treatment of Hunt[19], to absolute values of the slope greater than, or equal to, four. Despite the scarcity of data on the dependence of the agglomeration coefficient on the experimental conditions of crystallization, it is apparent that the effect of particle size in flow precipitation is counteracted by the effect of local supersaturation: as a result of imperfect mixing on the molecular scale, the supersturation around small particles, whose time of existence is still short, is greater than that around larger particles, where it has been relieved by mass transfer to the solid phase. The supersaturation of the solution surrounding the particles increases their tendency to agglomerate. Halfon and Kaliaguine[20], for example, found the agglomeration coefficient in crystallization of aluminium oxide trihydrate to be proportional to the fourth power of the solution supersaturation (and independent of the particle size). Another factor that could limit the effect of the particle size on the value of the agglomeration coefficient in the sense of Eq. (25), is the breakage of larger agglomerates in a turbulent mixing regime.

In most papers on the particle size distribution in continuous crystallizers with the particle size measured down to the micrometer range (Coulter counter, monochromatic light diffraction)[21–25], the plots of $\log n(L)$ *versus* L showed marked positive deviations from straight lines in the region of small particles. Such anomalies, which preclude accurate determination of the nucleation rate by the standard method (from the intercept of the semilogarithmic plot of the distribution on the $\log n(L)$ axis), have been explained in the literature in terms of a dependence of the crystal growth rate on the crystal size, nucleation of particles of finite size with the nucleation population function dependent on the nuclei size, or the phenomenon of the so-called growth dispersion (individual crystals of the same size grow at different rates under the same external conditions). Another possible factor here is agglomeration of small particles: by plotting published data[21–25] for the distribution in the form of $\log n(L)$ *versus* $\log L$, we obtain straight lines of slopes ranging from 2 to 4·5 in the region of small particles. In addition, crystals of aluminium potassium sulphate dodecahydrate[6] and calcium oxalate trihydrate[26] were found to agglomerate under conditions close to those used in some of the above studies[22,23,25] dealing with the same substances.

Agglomeration depends largely on the concentration of particles in suspension because it occurs by binary collisions which are proportional in number to the product of the concentrations of particles with the sizes considered. In contrast, the growth of individual particles as a result of transfer of the solute from the solution depends on the particle concentration only through the total surface area of the

particles and the mass balance for the solute. The effect of agglomeration on the particle size distribution is therefore largest for small particles, whose concentration is the highest. The distribution of larger particles is determined predominantly by the growth and the retention times of individual particles in the crystallizer. The size distribution for small particles is qualitatively described by the simple model presented in the theoretical part of this paper.

LIST OF SYMBOLS

$a = k_a \dot{N} \bar{t}^2$	dimensionless parameter
c	molar concentration of (equimolar) feed solutions (NL^{-3})
c_{eq}	equilibrium concentration of $CaCO_3$ in the mother liquor (NL^{-3})
F	Laplace transform of $f(v)$ function, see Eq. (*8*) (L^{-3})
$f(v)$	distribution function of particle volumes ($L^{-3} l^{-3}$)
k_a	agglomeration coefficient ($L^3 T^{-1}$)
L	characteristic dimension of particle (l)
L_0	characteristic dimension of primary particle (l)
L_{50}	median of $S(L)$ distribution (l)
L_{inflex}	coordinate of inflexion point in log $n(L)$ *versus* L plot, see Eq. (*17*) (l)
L_{max}	upper bound on linearity of log $n(L)$ *versus* log L plot (l)
$\dot{L}$	particle growth rate (lT^{-1})
$M(L)$	mass percent of particles of dimension larger than L
M_{CaCO_3}	molar mass of $CaCO_3$ (NM^{-1})
M_0	total number of particles in unit volume of suspension (L^{-3})
$\dot{N}$	nucleation rate of particles of volume v_0 *per* unit volume of suspension ($L^{-3} T^{-1}$)
$n(L)$	distribution function of characteristic particle dimensions ($L^{-3} l^{-1}$)
p	parameter of Laplace transform, see Eq. (*8*) (l^{-3})
q	auxiliary parameter defined by Eq. (*23*)
s	slope of log $n(L)$ *versus* log L plot
$S(L)$	proportion of surface area of particles of dimension smaller than L
$\bar{t}$	mean retention time of suspension in crystallizer (T)
u, v	particle volume (l^3)
v_0	volume of primary particle (l^3)
$\dot{v}$	rate of change of particle volume as a result of growth ($l^3\ T^{-1}$)
z	dimensionless parameter in Eq. (*21*)
$\delta(v)$	Dirac impulse function
ϱ_c	specific mass of crystals (Ml^{-3})

REFERENCES

1. Walton A. G.: *The Formation and Properties of Precipitates*, p. 175. Interscience, New York 1967.
2. Mullin J. W.: *Crystallisation*, p. 224. Butterworths, London 1972.
3. Misra C., White E. T.: J. Cryst. Growth *8*, 172 (1971).
4. Voigt H., Emons H.-H.: Freiberger Forschungshefte A600, *89* (1979).
5. Žáček S., Nývlt J., Karel M.: Chem. Prum. *31*, 630 (1981).
6. Kubota N., Mullin J. W.: J. Cryst. Growth *66*, 676 (1984).

7. Karel M., Nývlt J.: Cryst. Res. Technol. *20*, 447 (1985).
8. Smoluchowski M.: Z. Phys. Chem. *92*, 129 (1917).
9. Pulvermacher B., Ruckenstein E.: J. Colloid Interface Sci. *46*, 428 (1974).
10. Ramabhadran T. E., Peterson T. W., Seinfeld J. H.: AIChE J. *22*, 840 (1976).
11. Sastry K. V. S., Gaschignard P.: Ind. Eng. Chem., Fundam. *20*, 355 (1981).
12. Rosen J. M.: J. Colloid Interface Sci. *99*, 9 (1984).
13. Hendriks E. M., Spouge J. L., Eibl M., Schreckenberg M.: Z. Phys., B *58*, 219 (1985).
14. Friedlander S. K.: J. Meteorology *17*, 373 (1960).
15. Wray J. L., Daniels F.: J. Am. Chem. Soc. *79*, 2031 (1957).
16. Randolph A. D., Larson M. A.: *Theory of Particulate Processes*, p. 68. Academic Press, New York 1971.
17. Nakai T., Nakamaru H. in the book: *Industrial Crystallization 78* (E. J. de Jong and S. J. Jančić, Eds), p. 75. North Holland, Amsterdam 1979.
18. Saffman P. G., Turner J. S.: J. Fluid Mech. *1*, 16 (1956).
19. Hunt J. R. in the book: *Advances in Chemistry Series, No. 189, Particulates in Water* (M. C. Kavanaugh and J. O. Leckie, Eds), p. 243. American Chemical Society, Washington 1980.
20. Halfon A., Kaliaguine S.: Can. J. Chem. Eng. *54*, 168 (1976).
21. Youngquist G. R., Randolph A. D.: AIChE J. *18*, 421 (1972).
22. Jančić S. J., Garside J.: Chem. Eng. Sci. *30*, 1299 (1975).
23. Garside J., Jančić S. J.: AIChE J. *25*, 948 (1979).
24. Teodossiev N., Kirkova E. in the book: *Industrial Crystallization 84* (S. J. Jančić and E. J. de Jong, Eds), p. 305. Elsevier, Amsterdam 1984.
25. Brečević L., Garside J.: Chem. Eng. Sci. *36*, 867 (1981).
26. Škrtić D., Marković M., Füredi-Milhofer H. in the book: *Industrial Crystallization 84* (S. J. Jančić and E. J. de Jong, Eds), p. 421. Elsevier, Amsterdam 1984).

Translated by M. Škubalová.